

Making glue in high energy nuclear collisions

Alex Krasnitz* and Raju Venugopalan†

* *UCEH, Campus de Gambelas, Universidade do Algarve, Faro, P-8000, Portugal*¹

† *Physics Department, BNL, Upton, NY 11973*²

Abstract.

We discuss a real time, non-perturbative computation of the transverse dynamics of gluon fields at central rapidities in very high energy nuclear collisions.

INTRODUCTION

This year (1999) the Relativistic Heavy Ion Collider (RHIC) at Brookhaven will begin colliding beams of gold ions at center of mass energies of 200 GeV/nucleon. In slightly over 5 years from now, the LHC collider at CERN will do the same at center of mass energies of about 5.5 TeV/nucleon. At these energies, the appropriate basis to describe the colliding nuclei is that of partons, the quarks and gluons that constitute a nucleon, rather than a hadronic basis. An objective of the above mentioned experiments is to determine whether the partons, confined in nucleons prior to the collision, are liberated after the collision to form fleetingly, in the relatively large nuclear volume, an equilibrated state of matter popularly known as the quark gluon plasma.

Clearly, the space-time evolution, and possible equilibration, of matter produced in a nuclear collision must depend on the initial conditions. These are given by the parton distributions inside each of the nuclei. In perturbative QCD, the “factorized” expression for the multiplicity or energy distribution of a high p_t jet, with $p_t \approx \sqrt{s}$, is obtained by convolving the parton distributions in each of the nuclei, at the hard scale of interest, with the elementary parton-parton cross section. If $x \equiv p_t/\sqrt{s}$ is not too small, the factorized expression is reliable. With the measured nuclear structure functions, one can then compute the multiplicity and energy distributions of the jets produced [1].

¹) AK’s work supported by Portuguese Fundação para Ciência e a Tecnologia, grants CERN/S/FAE/1111/96 and CERN/P/FAE/1177/97

²) Invited talk by RV at the VIII Mexican School of Particles and Fields. RV’s work supported by DOE Nuclear Theory at BNL.

However, for $x \ll 1$ (corresponding to the transverse momentum range $\Lambda_{QCD} \ll p_t \ll \sqrt{s}$) the factorization formula for energy and multiplicity distributions breaks down. Simply put, this is because partons in one nucleus can resolve more than one parton in the other [2]. The parton densities in the nuclei become very large and may even saturate at sufficiently small x . The regime of high parton densities is a novel regime in QCD where, although the coupling constant may be small, the fields strengths are large enough for the physics to be non-perturbative [3].

The precise x value at which the above mentioned leading twist factorization breaks down is not clear. There are hints from from HERA that parton saturation is already seen in the data for $x \approx 10^{-4}$ and $Q^2 \approx 4 \text{ GeV}^2$ [4]. If this result is robust, similar effects may be seen in nuclei at larger values of x , even $x \sim 10^{-2}$. Their relevance for RHIC (and especially LHC) cannot then be ignored.

The effects of high parton densities in the central rapidity region of nuclear collisions can be studied in a model which is based on an effective field theory (EFT) approach to QCD at small x [5]. The model describes the time evolution of gauge fields in a nuclear collision. It takes into account, self-consistently, interference effects (which are also responsible for shadowing in deeply inelastic scattering) that become important at small x . Another nice feature is that it provides a space-time picture of the nuclear collision. This feature would be extremely useful if the gauge fields at late times were to provide the initial conditions for a parton cascade [6] or for hydrodynamic evolution if it can be determined that the matter produced has equilibrated [7].

The model is formulated in the infinite momentum frame $P^+ \rightarrow \infty$ and light cone gauge $A^+ = 0$. It contains a dimensionful parameter μ^2 , defined to be the color charge squared per unit area,

$$\mu^2 = \frac{A^{1/3}}{\pi r_0^2} \int_{x_0}^1 dx \left(\frac{1}{2N_c} q(x, Q^2) + \frac{N_c}{N_c^2 - 1} g(x, Q^2) \right). \quad (1)$$

Here q, g stand for the *nucleon* quark and gluon structure functions at the resolution scale Q of the physical process of interest. Also, above $x_0 = Q/\sqrt{s}$. Using the HERA structure function data, Gyulassy and McLerran [8] estimated that $\mu \leq 1 \text{ GeV}$ for LHC energies and $\mu \leq 0.5 \text{ GeV}$ at RHIC. Thus a window of applicability for weak coupling techniques does exist, and higher order calculations will tell us if it is smaller or larger than the simple classical estimate.

An interesting property of the light cone gauge is that final state interactions are absent! Kovchegov and Mueller [9] showed that the effects of final state interactions, as seen in a covariant gauge computation, are already contained in the nuclear wavefunction in light cone gauge. This non-trivial observation is at the heart of the approach described in this talk. Finally, we should alert the reader to alternative approaches to the one described here pursued in Refs. [10]– [11].

CLASSICAL MODEL OF GLUON PRODUCTION

At very high energies, the hard valence quark (and gluon) modes are highly Lorentz contracted, static sources of color charge for the wee parton, Weizsäcker–Williams, modes in the nuclei. The sources are described by the current

$$J^{\nu,a}(r_t) = \delta^{\nu+} \rho_1^a(r_t) \delta(x^-) + \delta^{\nu-} \rho_2^a(r_t) \delta(x^+), \quad (2)$$

where $\rho_{1(2)}$ correspond to the color charge densities of the hard modes in nucleus 1 (nucleus 2) respectively. The classical field describing the small x modes in the EFT is obtained by solving the Yang–Mills equations in the presence of the two sources. We have then

$$D_\mu F^{\mu\nu} = J^\nu. \quad (3)$$

The small x glue distribution is simply related to the Fourier transform $A_i^a(k_t)$ of the solution to the above equation by $\langle A_i^a(k_t) A_i^a(k_t) \rangle_\rho$.

The above averaging over the classical charge distributions is defined by

$$\langle O \rangle_\rho = \int d\rho_1 d\rho_2 O(\rho_1, \rho_2) \exp\left(-\int d^2r_t \frac{\text{Tr}[\rho_1^2(r_t) + \rho_2^2(r_t)]}{2g^4\mu^2}\right). \quad (4)$$

We have assumed identical nuclei with equal Gaussian weights $g^4\mu^2$.

Before the nuclei collide ($t < 0$), a solution of the equations of motion is

$$A^\pm = 0; \quad A^i = \theta(x^-)\theta(-x^+)\alpha_1^i(r_t) + \theta(x^+)\theta(-x^-)\alpha_2(r_t), \quad (5)$$

where $\alpha_q^i(r_t)$ ($q = 1, 2$ denote the labels of the nuclei and $i = 1, 2$ are the two transverse Lorentz indices) are *pure gauge* fields defined through the gauge transformation parameters $\Lambda_q(\eta, r_t)$ [8]

$$\alpha_q^i(r_t) = \frac{1}{i} \left(P e^{-i \int_{\pm\eta_{\text{proj}}}^0 d\eta' \Lambda_q(\eta', r_t)} \right) \nabla^i \left(P e^{i \int_{\pm\eta_{\text{proj}}}^0 d\eta' \Lambda_q(\eta', r_t)} \right). \quad (6)$$

Here $\eta = \pm\eta_{\text{proj}} \mp \log(x^\mp/x_{\text{proj}}^\mp)$ is the rapidity of the nucleus moving along the positive (negative) light cone with the gluon field $\alpha_{1(2)}^i$. The $\Lambda_q(\eta, r_t)$ are determined by the color charge distributions $\Delta_\perp \Lambda_q = \rho_q$ ($q=1,2$) with Δ_\perp being the Laplacian in the perpendicular plane.

For $t > 0$ the solution is no longer pure gauge. Working in the Schwinger gauge $A^\tau \equiv x^+ A^- + x^- A^+ = 0$, Kovner, McLerran and Weigert [12] found that with the ansatz

$$A^\pm = \pm x^\pm \alpha(\tau, r_t); \quad A^i = \alpha_\perp^i(\tau, r_t), \quad (7)$$

where $\tau = \sqrt{2x^+x^-}$, Eq. 3 could be written more simply in terms of α and α_\perp . Note that these fields are independent of η —the solutions are explicitly boost invariant in the forward light cone!

The initial conditions for the fields $\alpha(\tau, r_t)$ and α_\perp^i at $\tau = 0$ are obtained by matching the equations of motion (Eq. 3) at the point $x^\pm = 0$ and along the boundaries $x^+ = 0, x^- > 0$ and $x^- = 0, x^+ > 0$. Remarkably, for such singular sources, there exist a set of non-singular initial conditions for the smooth evolution of the classical fields in the forward light cone. One obtains

$$\alpha_\perp^i|_{\tau=0} = \alpha_1^i + \alpha_2^i ; \alpha|_{\tau=0} = \frac{i}{2}[\alpha_1^i, \alpha_2^i]. \quad (8)$$

Gyulassy and McLerran have shown [8] that even when the fields $\alpha_{1,2}^i$ before the collision are smeared out in rapidity, to properly account for singular contact terms in the equations of motion, the above boundary conditions remain unchanged. Further, since as mentioned the equations are very singular at $\tau = 0$, the only condition on the derivatives of the fields that would lead to regular solutions are $\partial_\tau \alpha|_{\tau=0}, \partial_\tau \alpha_\perp^i|_{\tau=0} = 0$.

Perturbative solutions of the Yang-Mills equations to order ρ^2 in the color charge density (or equivalently to second order in $\alpha_S \mu/k_t$) were found, and at late times, after averaging over the Gaussian sources, the number distribution of classical gluons was found to be [12,8,13,14]

$$\frac{dN}{dyd^2k_t} = \pi R^2 \frac{2g^6 \mu^4 N_c(N_c^2 - 1)}{(2\pi)^4 k_t^4} L(k_t, \lambda), \quad (9)$$

where $L(k_t, \lambda)$ is an infrared divergent function at the scale λ . This result agrees with the quantum bremsstrahlung formula of Gunion and Bertsch [15]. Also, Guo has shown that the above result is equivalent to the perturbative QCD factorized result for the process $qq \rightarrow qqg$ [16].

From the above expression, it is clear that distributions are very sensitive to $L(k_t, \lambda)$. Usually, as in Gunion and Bertsch, this divergence is absorbed in a non-perturbative form factor. What is novel about the classical approach is that, at sufficiently high energies, the non-linearities in the Yang-Mills fields self-consistently regulate this infrared divergence. To confirm this claim, one needs to solve the Yang-Mills equations to all orders in $\alpha_S \mu/k_t$. A non-perturbative solution of the Yang-Mills equations on a two dimensional transverse lattice was performed by us [17] and is described below.

REAL TIME SIMULATIONS OF YANG-MILLS I: LATTICE FORMULATION

We have seen above that the Yang-Mills equations are boost invariant. This is a consequence of the sources being δ -functions on the light cone- the nuclei are assumed to move with the speed of light! Since this is not the case, boost invariance is only approximate. It should, however, be a good assumption at the energies of interest-especially at central rapidities.

The boost invariance assumption simplifies our numerical work considerably. We now have a 2+1-dimensional theory and all the dynamics is restricted to the transverse plane (we assume $\eta = 0$). The Yang–Mills equations are most conveniently solved by fixing $A^\tau = 0$ gauge and solving Hamilton’s equations. Gauge invariance is ensured by defining the theory, in the usual way, on a 2-dimensional transverse lattice. The lattice Hamiltonian is the Kogut-Susskind Hamiltonian for gauge fields coupled to an adjoint scalar

$$H_L = \frac{1}{2\tau} \sum_{l \equiv (j, \hat{n})} E_l^a E_l^a + \tau \sum_{\square} \left(1 - \frac{1}{2} \text{Tr} U_{\square} \right),$$

$$+ \frac{1}{4\tau} \sum_{j, \hat{n}} \text{Tr} \left(\Phi_j - U_{j, \hat{n}} \Phi_{j+\hat{n}} U_{j, \hat{n}}^\dagger \right)^2 + \frac{\tau}{4} \sum_j \text{Tr} p_j^2, \quad (10)$$

where E_l are generators of right covariant derivatives on the group and $U_{j, \hat{n}}$ is a component of the usual SU(2) matrices corresponding to a link from the site j in the direction \hat{n} . The first two terms correspond to the contributions to the Hamiltonian from the chromoelectric and chromomagnetic field strengths respectively. Also, above $\Phi \equiv \Phi^a \sigma^a$ is the adjoint scalar field with its conjugate momentum $p \equiv p^a \sigma^a$.

Lattice equations of motion follow directly from H_L of Eq. 10. For any dynamical variable v , with no explicit time dependence, $\dot{v} = \{H_L, v\}$, where \dot{v} is the derivative with respect to τ , and $\{\}$ denote Poisson brackets. We take E_l , U_l , p_j , and Φ_j as independent dynamical variables, whose only nonvanishing Poisson brackets are $\{p_i^a, \Phi_j^b\} = \delta_{ij} \delta_{ab}$; $\{E_l^a, U_m\} = -i \delta_{lm} U_l \sigma^a$; $\{E_l^a, E_m^b\} = 2 \delta_{lm} \epsilon_{abc} E_l^c$ (no summing of repeated indices). The equations of motion are consistent with a set of local constraints (Gauss’ laws). Their evolution in τ after the nuclear collision is determined by Hamilton’s equations and their values at the initial time $\tau = 0$.

The initial conditions on the lattice are the constraints on the longitudinal gauge potential A^\pm and the transverse link matrices U_\perp at $\tau = 0$. The longitudinal gauge potentials are zero outside the light cone and satisfy the Schwinger gauge condition $A^\tau = 0$ inside the light cone $x_\pm > 0$. They can be written, as in the continuum case (see Eq. 7), as

$$A^\pm = \pm x^\pm \theta(x^+) \theta(x^-) \alpha(\tau, x_t). \quad (11)$$

The transverse link matrices are, for each nucleus, pure gauges before the collision. This fact is reflected by writing

$$U_\perp = \theta(-x^+) \theta(-x^-) I + \theta(x^+) \theta(x^-) U(\tau) + \theta(-x^+) \theta(x^-) U_1 + \theta(x^+) \theta(-x^-) U_2, \quad (12)$$

where $U_{1,2}$ are pure gauge.

The pure gauges are defined on the lattice as follows. To each lattice site j we assign two SU(N_c) matrices $V_{1,j}$ and $V_{2,j}$. Each of these two defines a pure gauge lattice gauge configuration with the link variables $U_{j, \hat{n}}^q = V_{q,j} V_{q,j+\hat{n}}^\dagger$ where

$q = 1, 2$ labels the two nuclei. Also, as in the continuum, the gauge transformation matrices $V_{q,j}$ are determined by the color charge distribution $\rho_{q,j}$ of the nuclei, normally distributed with the standard deviation $g^4 \mu_L^2$:

$$P[\rho_q] \propto \exp\left(-\frac{1}{2g^4 \mu_L^2} \sum_j \rho_{q,j}^2\right). \quad (13)$$

Parametrizing $V_{q,j}$ as $\exp(i\Lambda_j^q)$ with Hermitean traceless Λ_j^q , we then obtain Λ_j^q by solving the lattice Poisson equation

$$\Delta_L \Lambda_j^q \equiv \sum_n \left(\Lambda_{j+n}^q + \Lambda_{j-n}^q - 2\Lambda_j^q\right) = \rho_{q,j}. \quad (14)$$

The correct continuum solution (Eqs. 5 and 7) for the transverse fields A_\perp is recovered by taking the formal continuum limit of Eq. 12.

Using the general representation of the gauge fields in Eqs. 11 and 12, we shall now state the initial conditions for them at $\tau = 0$.

$$\begin{aligned} U_\perp|_{\tau=0} &= (U_1 + U_2)(U_1^\dagger + U_2^\dagger)^{-1}; \quad E_l|_{\tau=0} = 0. \\ p_j|_{\tau=0} &= 2\alpha; \quad \Phi_j = 0, \end{aligned} \quad (15)$$

where U_\perp is defined as $\exp(ia_\perp \alpha_\perp)$. The above initial conditions are obtained by matching the lattice equations of motion in the four light cone regions at $\tau = 0$. For details we refer the reader to Ref. [17].

REAL TIME SIMULATIONS OF YANG–MILLS II: DISCUSSION OF RESULTS

In Ref. [17], we reported results of simulations of the time evolution of classical fields in a 2+1-dimensional SU(2) gauge theory described by the Hamiltonian in Eq. 10. The simulations were carried out on transverse lattices ranging from 20×20 sites to 160×160 sites. The lattice results depend on one dimensionless parameter, $g^2 \mu L$ [18]. The parameter L corresponds to the size of the nucleus; μ defined in Eq. (1) is determined by the size of the nucleus, the energy of the nucleus, and the hard scale Q of interest; the strong coupling g runs as a function of either Q or μ depending on which is greater.

Thus, once given the energy and size of the incoming nuclei, and the hard scale of interest, we can determine the evolution of gauge fields in the central rapidity region. Consider, for instance, colliding two gold nuclei ($A \sim 200$) at RHIC and LHC energies. Approximating $L^2 = \pi R^2$, we obtain $L = 11.6$ fm. For the hard scales of interest, $Q \approx 1\text{--}2$ GeV, $\mu \sim 0.5$ GeV at RHIC ($\mu \sim 1$ GeV at LHC). One then obtains

$$\begin{aligned} g^2 \mu L &\approx 120 \quad (\text{RHIC}) \\ &\approx 240 \quad (\text{LHC}). \end{aligned} \quad (16)$$

Above we have chosen $g = 2$ (or equivalently, $\alpha_S \approx 0.3$).

On the lattice, the lattice coupling is $g^2(\mu a)(L/a) \equiv g^2\mu_L N$. The continuum limit is obtained by keeping $g^2\mu_L N$ fixed (to the physical value of interest—as in Eq. 16) and taking μ_L to zero. It appears from our simulations that we are in the weak coupling regime for $\mu_L = 0.017, 0.035$ in lattice units. For the physical values of $g^2\mu L$ above, these would correspond to lattices an order of magnitude larger than those considered so far. Detailed simulations on the above physical scenario will be reported at a later date.

We now turn to an issue of some concern; whether quantities of interest have a continuum limit (in the above defined sense) in the classical theory. For instance, in thermal field theories, it is not clear that dynamical quantities such as auto-correlation functions have a well defined limit as the lattice spacing $a \rightarrow 0$. In the EFT described here, there is reason to be more optimistic.

Consider the following gauge invariant quantity; the energy density $p^a p^a = E_k/N^2$ of the scalar field on the lattice (in units of μ_L^4). It is plotted as a function of the lattice size N (in units of the lattice spacing) in Fig. 1 for $\mu_L = 0.0177, 0.035$.

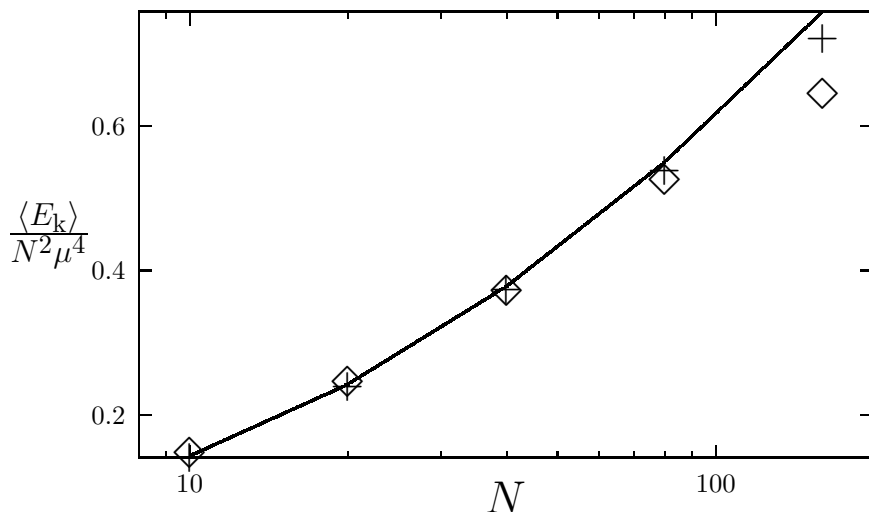


FIGURE 1. The lattice size dependence of the scalar kinetic energy density, expressed in units of μ^4 for $\mu = 0.0177$ (pluses) and $\mu = 0.035$ (diamonds). The solid line is the LPT prediction. The error bars are smaller than the plotting symbols.

The solid line is the prediction from lattice perturbation theory (LPT). It is given by

$$p^a p^a = 6 \left(\frac{\mu}{N} \right)^4 \sum_{n,n'} \left[\left(\sum_{\vec{k}} \frac{\sin(l_n) \sin(l_{n'})}{\Delta^2(l)} \right)^2 + 16 \left(\sum_{\vec{k}} \frac{\sin^2(\frac{l_n}{2}) \sin^2(\frac{l_{n'}}{2})}{\Delta^2(l)} \right)^2 \right], \quad (17)$$

where $l_n = 2\pi n/N$ and $\Delta(l) = 2 \sum_{n=1,2} (1 - \cos(l_n))$ is the usual lattice Laplacian. The continuum limit of the above equation has the form $p^a p^a \rightarrow A + B \log^2(L/a)$, where A and B are constants that can be determined from the above equation.

From Fig. 1, it can be seen that the kinetic energy density diverges as $\log^2(L/a)$ —i.e., it does not have a well-defined continuum limit. This divergence is softer than in a thermal theory, where the energy density diverges as an inverse power of the lattice spacing. If we subtract the perturbative result in Eq. 17 at some scale $\Lambda_{nonpert}$, the resulting expression will have a continuum limit but will depend on $\Lambda_{nonpert}$. The trick is to find a $\Lambda_{nonpert}$ for which the contribution to the “non-perturbative” scalar kinetic energy density converges as $\mu_L \rightarrow 0$. In Table. 1, we show the results, at $\tau = 0$, of simulations where $g^2\mu L = 33.6$ is kept fixed (note: here we fix $g = 1$). The lattice cut-offs (recall that $k_t = 2\pi n/L$) of $n_{cut} = 10, 15, 20$ correspond to $\Lambda_{nonpert} = 1.08, 1.62, 2.16$ GeV respectively. For $n_{cut} =$

TABLE 1. Scalar k.e. density $\frac{E_k}{N^2\mu^4}$ vs μ_L for fixed $g^2\mu L = 33.6$. Columns 3–5 are the scalar.ke.d after subtracting LPT.h. contribution for $n > n_{cut}$ in Eq. 17.

μ_L	$\frac{E_k}{N^2\mu^4}$	$n_{cut}=10$	$n_{cut}=15$	$n_{cut}=20$
.84	07.24e-02	.0341	.0562	.0702
.56	10.20e-02	.0407	.0636	.0791
.42	12.38e-02	.0426	.0694	.0852
.21	17.60e-02	.0268	.0702	.0945

15, the non-perturbative contribution to the scalar.ke.density appears to converge to a constant value as μ_L is decreased, keeping $g^2\mu L$ fixed. This result must of course be confirmed for larger lattices and other values of $g^2\mu L$. Caveat aside, our results appear to suggest that for a particular $\Lambda_{nonpert}$ there is a non-perturbative contribution to the energy density that survives in the continuum limit.

Presumably, the subtraction described above may also be performed for static quantities in a thermal field theory. It is unlikely that this procedure there is reliable for dynamic quantities. In our case, the scalar kinetic energy is a dynamic quantity evolving in time. If the above mentioned procedure is to be use, it must also be valid at later times. We are optimistic that this may be the case because our simulations suggest that the time evolution of hard modes decouples from that of the soft modes. This is illustrated very clearly by Fig. 2 of the most recent of our papers cited in Ref. [17].

The parameter $\Lambda_{nonpert}$ may be given a physical interpretation. At sufficiently high energies, one may be able to relate it to the physical scale at which one begins to see deviations from perturbative predictions (note: at very high energies one expects $\Lambda_{nonpert} \gg \Lambda_{QCD}$) due to high parton density effects.

We are currently studying whether the non-perturbative contribution to the scalar energy density also has a robust continuum limit at late times [19].

REFERENCES

1. K. Kajantie, P. V. Landshoff, and J. Lindfors, *Phys. Rev. Lett.* **59** (1987) 2527; K. J. Eskola, K. Kajantie, and J. Lindfors, *Nucl. Phys.* **323** (1989) 37; J.-P. Blaizot and A. H. Mueller, *Nucl. Phys.* **B289** (1987)847; K. J. Eskola, *Comments in Nucl. and Part. Phys.* **22** (1998) 185.
2. R. Venugopalan, *Comments in Nucl. and Part. Physics*, **22** (1998) 113.
3. L. V. Gribov, E. M. Levin, and M. G. Ryskin, *Phys. Repts.* 1 (1983); A. H. Mueller and J. Qiu, *Nucl. Phys.* **B268** 427 (1986).
4. A. H. Mueller, hep-ph/9904404, hep-ph/9902302.
5. L. McLerran and R. Venugopalan, *Phys. Rev.* **D49** 2233 (1994); **D49** 3352 (1994); **50** 2225 (1994); J. Jalilian–Marian, A. Kovner, L. McLerran and H. Weigert, *Phys. Rev.* **D55** 5414 (1997); J. Jalilian–Marian, A. Kovner, A. Leonidov and H. Weigert, *Nucl. Phys.* **B504** (1997) 415; *Phys. Rev.* **D59** (1999) 034007; J. Jalilian–Marian, A. Kovner and H. Weigert, *Phys. Rev.* **D59** (1999) 014015.
6. K. Geiger, *Phys.Rep.* **258** 237 (1995); X.-N. Wang, *Phys. Rep.* **280** 287 (1997).
7. J. D. Bjorken, *Phys.Rev.* **D27** 140 (1983); J. Sollfrank, P. Houvinen, M. Kataja, P. V. Ruuskanen, M. Prakash and R. Venugopalan, *Phys. Rev.* **C55** 392 (1997).
8. M. Gyulassy and L. McLerran, *Phys. Rev.* **C56** (1997) 2219.
9. Y. Kovchegov and A. H. Mueller *Nucl. Phys.* **B529** 451 (1998).
10. S. A. Bass, B. Müller, and W. Poschl, nucl-th/9808011; B. Müller and W. Poschl, nucl-th/9808031, nucl-th/9812066.
11. A. Makhlin and E. Surdutovich, *Phys. Rev.* **C58** 389 (1998).
12. A. Kovner, L. McLerran and H. Weigert, *Phys. Rev* **D52** 3809 (1995); **D52** 6231 (1995).
13. Y. V. Kovchegov and D. H. Rischke, *Phys. Rev.* **C56** (1997) 1084.
14. S. G. Matinyan, B. Müller and D. H. Rischke, *Phys. Rev.* **C56** (1997) 2191; *Phys. Rev.* **C57** (1998) 1927.
15. J. F. Gunion and G. Bertsch, *Phys. Rev.* **D25** 746 (1982).
16. X. Guo, *Phys. Rev.* **D59** 094017 (1999).
17. A. Krasnitz and R. Venugopalan, hep-ph/9706329, hep-ph/9808332, hep-ph/9809433.
18. R. V. Gavai and R. Venugopalan, *Phys. Rev.* **D54** 5795 (1996).
19. A. Krasnitz and R. Venugopalan, in progress.